

CrystEngComm

Accepted Manuscript



This is an *Accepted Manuscript*, which has been through the Royal Society of Chemistry peer review process and has been accepted for publication.

Accepted Manuscripts are published online shortly after acceptance, before technical editing, formatting and proof reading. Using this free service, authors can make their results available to the community, in citable form, before we publish the edited article. We will replace this *Accepted Manuscript* with the edited and formatted *Advance Article* as soon as it is available.

You can find more information about *Accepted Manuscripts* in the [Information for Authors](#).

Please note that technical editing may introduce minor changes to the text and/or graphics, which may alter content. The journal's standard [Terms & Conditions](#) and the [Ethical guidelines](#) still apply. In no event shall the Royal Society of Chemistry be held responsible for any errors or omissions in this *Accepted Manuscript* or any consequences arising from the use of any information it contains.

ARTICLE

Influence of the Cation Size on the Second Harmonic Generation Response of Chiral $A(\text{VO}_2)_2(\text{PO}_4)\cdot 3\text{H}_2\text{O}$ ($A = \text{K}^+, \text{NH}_4^+$ and Rb^+)

Cite this: DOI: 10.1039/x0xx00000x

Received 00th January 2012,
Accepted 00th January 2012

DOI: 10.1039/x0xx00000x

www.rsc.org/R. Gautier^{a,b,*}, S. Auguste^a, S. Clevers^c, V. Dupray^c, G. Coquerel^c and E. Le Fur^{a,*}

New insights on the relationships between chirality and nonlinear optical (NLO) properties are of interest for the future design of phases with strong Second Harmonic Generation (SHG) response. The structures of the new $A(\text{VO}_2)_2(\text{PO}_4)\cdot 3\text{H}_2\text{O}$ ($A = \text{K}^+$ and Rb^+) phases prepared by hydrothermal method were determined by single crystal X-ray diffraction. The SHG properties of these new chiral materials and the previously reported isostructural $\text{NH}_4(\text{VO}_2)_2(\text{PO}_4)\cdot 3\text{H}_2\text{O}$ were measured. For an incident wavelength of 1064 nm, the SHG responses at 532 nm of Rb, NH_4 and K analogues were respectively 2, 6 and 24 times stronger than quartz. The NLO properties were shown to increase strongly when the structure slightly contracts.

INTRODUCTION

Chiral materials are of interest owing to their physical properties such as dichroism or Second Harmonic Generation (SHG) activity. In the past decades, more attention has been focused on developing new strategies for the design of noncentrosymmetric (NCS) compounds with strong SHG response. In order to develop these strategies, one should firstly be able to identify the characteristics of the material which enhance the response.

In the literature, different features have been reported to play a role in the SHG efficiency. Thus, Ye *et al.* showed that the SHG response was correlated with the alignment of polar anionic units.¹ They calculated this alignment for different NCS materials and were able to predict the ones exhibiting high response. Then, this optimization of the alignment was a goal for different research groups trying to design new polar materials. Different strategies which enable this design were reported such as the use of Λ shape units or hydrogen bondings.²⁻¹⁰ Other structural features were shown to play a role in the optimization of NLO properties. Thus, the dimensionality of the crystal structure and the polarizability of alkali metal can influence these properties. For example, Bera *et al.* showed an enhancement of the SHG response when increasing x in $\text{Li}_{1-x}\text{Na}_x\text{AsS}_2$ (Na has a higher polarizability than Li).¹¹ In AAsSe_2 ($A = \text{Li}, \text{Na}, \dots$), controlling the dimensionality is presented as a strategy to design better SHG materials.¹² The distortion of a NCS structure from the CS equivalent was also shown to be

correlated to the SHG response.¹³ This quantification is similar to the previously reported approach to evaluate the chirality degree of a molecule and has been successful to explain the strong SHG response of borate compounds.¹⁴

In this context, it is important to note that most of the approaches to understand the relationships between crystal structure and SHG response have been focused on inorganic *polar* materials. The inorganic *chiral* materials have been much less studied and the structural parameters influencing the SHG response are not well understood.

In order to provide more insights on the relationships between chirality and nonlinear optical (NLO) properties, we targeted the synthesis of new $A(\text{VO}_2)_2(\text{PO}_4)\cdot 3\text{H}_2\text{O}$ ($A =$ alkali metal) isostructural of the previously reported chiral $\text{NH}_4(\text{VO}_2)_2(\text{PO}_4)\cdot 3\text{H}_2\text{O}$.¹⁵ These materials exhibit different SHG responses and serve to a better understanding of the structural parameters influencing the NLO properties.

EXPERIMENTAL DETAILS

Synthesis

$\text{K}(\text{VO}_2)_2\text{PO}_4\cdot 3\text{H}_2\text{O}$ and $\text{Rb}(\text{VO}_2)_2\text{PO}_4\cdot 3\text{H}_2\text{O}$ crystals were prepared by hydrothermal method. The mixture is composed of 1mmol V_2O_5 , 2mmol M_2CO_3 (with $\text{M} = \text{K}^+$ and Rb^+), 1ml H_3PO_4 85% and 4ml H_2O . To prepare samples suitable for single crystal X-ray diffraction, the reactants were loaded in a Teflon-

lined stainless steel autoclave (23ml) and heated at 100°C during 25h and cooled down to room temperature (5°C/h). The crystals were washed with cold water and dried in a desiccator. Layer green crystals of $A_x(\text{VOPO}_4)_y\text{H}_2\text{O}$ were also obtained during hydrothermal synthesis. In order to prepare pure polycrystalline $A(\text{VO}_2)_2\text{PO}_4 \cdot 3\text{H}_2\text{O}$ samples, the mixture of reactants was refluxed under agitation during 30 min instead of realizing hydrothermal synthesis (Figure S1).

Structure determination

The crystal structures of $\text{K}(\text{VO}_2)_2\text{PO}_4 \cdot 3\text{H}_2\text{O}$ and $\text{Rb}(\text{VO}_2)_2\text{PO}_4 \cdot 3\text{H}_2\text{O}$ were solved using a four-circle Nonius KappaCCD diffractometer with a graphite monochromated $\text{Mo K}\alpha$ radiation ($\lambda=0.71073\text{\AA}$). The intensities were collected through the program COLLECT for the Kappa CCD¹⁶ in the ω - ϕ scanning mode. Using WINGX software,¹⁷ the structures were solved with SIR-97¹⁸ and refined with SHELXL-97.¹⁹

| | $\text{K}(\text{VO}_2)_2(\text{PO}_4) \cdot 3\text{H}_2\text{O}$ | $\text{Rb}(\text{VO}_2)_2(\text{PO}_4) \cdot 3\text{H}_2\text{O}$ |
|--|--|---|
| Chemical formula | $\text{K}(\text{VO}_2)_2(\text{PO}_4) \cdot 3\text{H}_2\text{O}$ | $\text{Rb}(\text{VO}_2)_2(\text{PO}_4) \cdot 3\text{H}_2\text{O}$ |
| Chemical formula weight (g.mol ⁻¹) | 353.95 | 400.32 |
| Crystal system | Orthorhombic | Orthorhombic |
| Space group | $P2_12_12_1$ | $P2_12_12_1$ |
| Z | 4 | 4 |
| a (Å) | 7.1203(1) | 7.1884(2) |
| b (Å) | 10.1782(2) | 10.3290(3) |
| c (Å) | 12.3477(3) | 12.3618(4) |
| V (Å ³) | 894.86(3) | 917.85(5) |
| T (K) | 293(2) | 293(2) |
| Maximum 2 θ | 64° | 55° |
| $\lambda(\text{Mo K}\alpha)$ (Å) | 0.71073 | 0.71073 |
| Unique data after merging | 3096 | 2103 |
| Observed data (>2.0 $\sigma(F^2)$) | 2950 | 1815 |
| Free parameters | 136 | 137 |
| Data collected | h : -10, 10 k : -14, 15 l : -18, 16 | h : -9, 8 k : -13, 13 l : -16, 15 |
| $\rho_{\text{calc.}}$ (g.cm ⁻³) | 2.458 | 2.820 |
| Absorption coefficient | 2.208 cm ⁻¹ | 8.183 cm ⁻¹ |
| R _{int} | 0.024 | 0.071 |
| R ₁ | 0.026 | 0.039 |
| wR ₂ | 0.069 | 0.075 |
| Goodness-of-fit | 1.22 | 1.16 |
| Min, Max (e/Å ³) | -0.55, 0.63 | -0.70, 1.01 |

Table 1. Crystal data for $\text{K}(\text{VO}_2)_2(\text{PO}_4) \cdot 3\text{H}_2\text{O}$ and $\text{Rb}(\text{VO}_2)_2(\text{PO}_4) \cdot 3\text{H}_2\text{O}$

Thermal analysis

Thermogravimetric and Differential Scanning Calorimetry (DSC) measurements were monitored on a SETARAM TG-DSC111 instrument under pure argon from room temperature to 800°C with an heating rate of 5°C/min.

Particle-size distribution analysis

The analysis of the particle-size distribution was performed by laser diffraction. The samples of $A(\text{VO}_2)_2(\text{PO}_4) \cdot 3\text{H}_2\text{O}$ ($A=\text{K}^+$, NH_4^+ and Rb^+) were dispersed in ethanol solution. A Beckman-Coulter LS-230 apparatus equipped with a 750 nm laser beam was used to measure the diameter of the particles with sizes ranging from 0.4 μm to 2000 μm .

UV-Visible diffuse reflectance

Diffuse reflectance spectra were collected from 350 nm to 1000 nm for compounds $A(\text{VO}_2)_2(\text{PO}_4) \cdot 3\text{H}_2\text{O}$ ($A=\text{K}^+$, NH_4^+ and Rb^+) on a Varian Cary 5G spectrophotometer equipped with a 60 mm integrating sphere. The samples were prepared by finely grinding the materials in a mortar. The absorption data (a/S) were calculated from the reflectance data with the use of the Kubelka-Munk function ($a/S = (1-R)^2/2R$) where a is the absorption coefficient, S is the scattering coefficient, and R is the reflectance.

Second Harmonic Generation measurements

Figure 1 shows the experimental setup used for the TR-SHG measurements. A Nd:YAG Q-switched laser (Quantel) operating at 1.06 μm was used to deliver up to 360 mJ pulses of 5 ns duration with a repetition rate of 10 Hz. An energy adjustment device made up of two polarizers (P) and a half-wave plate ($\lambda/2$) allowed the incident energy to vary from 10 to ca. 312 mJ per pulse. A RG1000 filter was used after the energy adjustment device to remove light from laser flash lamps. The samples (few mg of powder in a crucible) were placed in a computer controlled Heating-Cooling stage (Linkam THMS-600) and were irradiated with a beam (4 mm in diameter). The signal generated by the sample (diffused light) was collected into an optical fiber (500 μm of core diameter) and directed onto the entrance slit of a spectrometer (Ocean Optics). A boxcar integrator allowed an average spectrum (spectral range 490-590 nm) with a resolution of 0.1 nm to be recorded over 3 s (30 pulses).

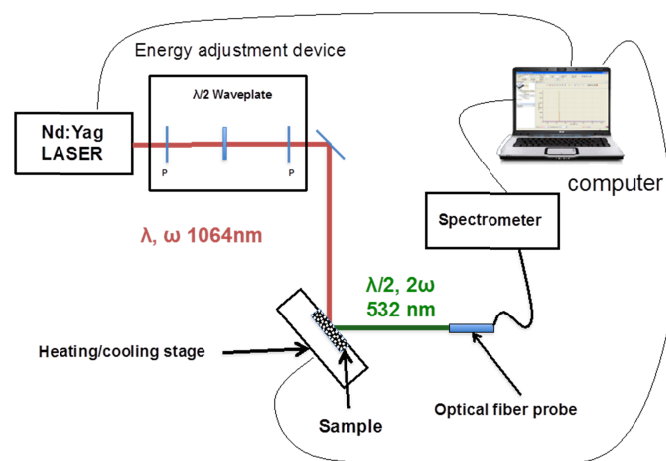


Figure 1. Experimental setup Second Harmonic Generation Apparatus constituted of Nd:YAG Q-switched laser operating at 1064 nm.

According to Kurtz and Perry SHG powder method, SHG signal intensities were compared to the signal of a reference compound (α -quartz powder- 45 μm average size).²⁰ As the synthesized materials undergo slight degradation, the SHG measurements were performed at 80K and the incident energy was set at the minimum intensity.

RESULTS AND DISCUSSION

Structure description

The isostructural $A(\text{VO}_2)_2(\text{PO}_4)\cdot 3\text{H}_2\text{O}$ ($A=\text{K}^+$, NH_4^+ and Rb^+) materials crystallize in the chiral space-group $P2_12_12_1$. The structure is built of vanadium oxide chains running along the a axis and connected by phosphate groups (Figure 2). The alkali metals and free water molecules are localized inside of the channels. In the chains, $\text{V}(1)\text{O}_6$ and $\text{V}(2)\text{O}_6$ corner-sharing octahedra form trimer fragments. The V-O bond lengths in $\text{V}(1)\text{O}_6$ octahedra range from 1.6068(21) Å/ 1.5968(43) Å to 2.2490(21) Å/ 2.2675(44) Å for $A=\text{K}/\text{Rb}$, respectively. The two shortest V=O bonds are terminal. In $\text{V}(2)\text{O}_6$ octahedra, the bond distances range from 1.6524(43) Å/ 1.6519 (11) Å to 2.2045(20) Å/ 2.2220(42) Å for $A=\text{K}/\text{Rb}$, respectively. One of the two shortest bonds corresponds to a terminal oxide ligand whereas the other one alternates with a long V-O bond along the chains. The volume of the unit cells increase with the size of the cations such as $\text{K}^+ < \text{NH}_4^+ < \text{Rb}^+$ ($V/Z = 223.71 \text{ \AA}^3$, 228.5 \AA^3 and 229.46 \AA^3 , respectively).

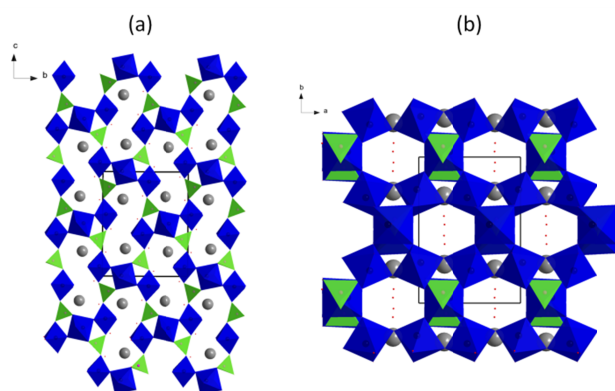


Figure 2. Crystal structures of $A(\text{VO}_2)_2(\text{PO}_4)\cdot 3\text{H}_2\text{O}$ ($A=\text{K}^+$, NH_4^+ and Rb^+) compounds viewed (a) along a and (b) along c . Phosphates and vanadium oxides groups are represented in green and blue color, respectively.

Thermal behaviour of $A(\text{VO}_2)_2(\text{PO}_4)\cdot 3\text{H}_2\text{O}$ ($A=\text{K}^+$, NH_4^+ and Rb^+)

The thermogravimetric analysis and Differential Scanning Calorimetry performed on $A(\text{VO}_2)_2(\text{PO}_4)\cdot 3\text{H}_2\text{O}$ ($A=\text{K}^+$, NH_4^+ and Rb^+) phases show a weight loss between room temperature and 170°C accompanied by an endothermic peak in the DSC curve corresponding to the dehydration of the materials (loss of

three water molecules) (Figure 3). The melting process of the anhydrous phases is identified by another endothermic peak for potassium and rubidium vanadium phosphate phases at 520°C. For $\text{NH}_4(\text{VO}_2)_2(\text{PO}_4)\cdot 3\text{H}_2\text{O}$, a second weight variation corresponding to the loss of NH_3 and $\frac{1}{2} \text{H}_2\text{O}$ is observed at 330°C. This weight loss is in agreement with the previous transformation of $\text{NH}_4(\text{VO}_2)_2(\text{PO}_4)\cdot 3\text{H}_2\text{O}$ into $(\text{VO})_2\text{P}_2\text{O}_7$ and amorphous phase at about 400°C under ammoxidation conditions.¹⁵

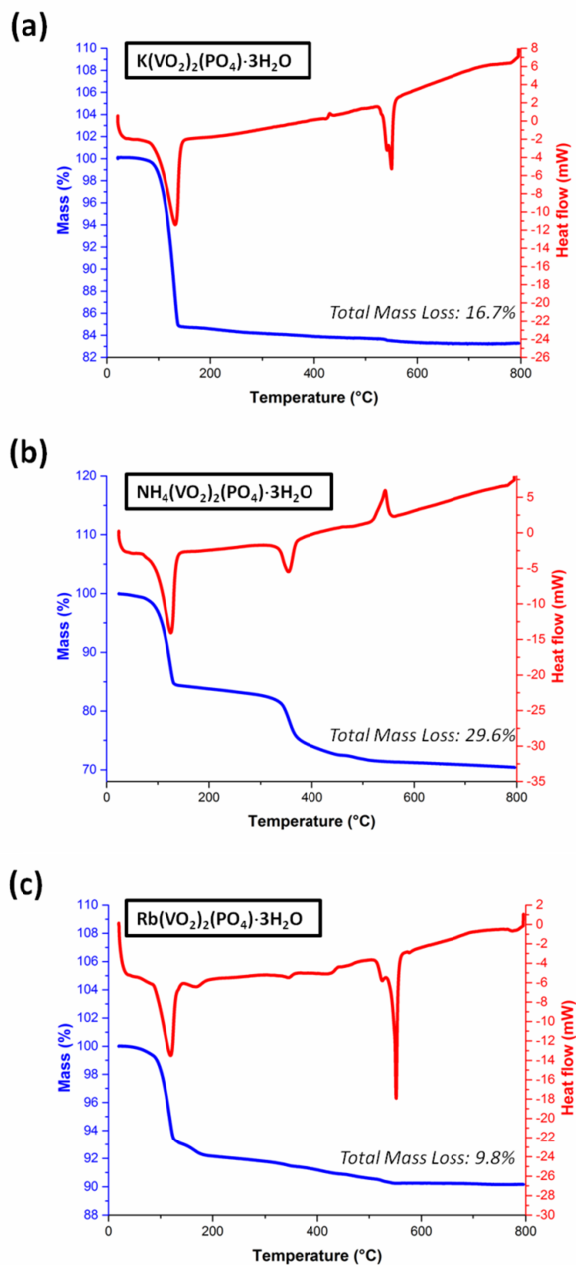


Figure 3. Thermogravimetric analysis and Differential Scanning Calorimetry of (a) $\text{K}(\text{VO}_2)_2(\text{PO}_4)\cdot 3\text{H}_2\text{O}$ (6.6 mg) (Expected weight loss: 15.2%), (b) $\text{NH}_4(\text{VO}_2)_2(\text{PO}_4)\cdot 3\text{H}_2\text{O}$ (8 mg) (Expected weight loss: 24.02%) and (c) $\text{Rb}(\text{VO}_2)_2(\text{PO}_4)\cdot 3\text{H}_2\text{O}$ (12.7 mg) compounds under Argon.

Influence of the cation size on the SHG properties

As the $A(\text{VO}_2)_2(\text{PO}_4)\cdot 3\text{H}_2\text{O}$ ($A=\text{K}^+$, NH_4^+ and Rb^+) materials crystallize in the space-group $P2_12_12_1$, these phases are potentially SHG active (every chiral compounds except the ones in the point-group 432 can be active).²¹ The crystal size distributions are similar for every compounds. Thus, the average size is about 18 μm , 25 μm and 32 μm for the K, Rb and NH_4 analogues, respectively (Figure S2). Moreover, UV-Vis diffuse reflectance spectra show that the compounds have similar absorption at the frequency of the second harmonic (532 nm) (Figure 4) and the three samples show similar crystallinity. These results allow a fair comparison between the SHG responses of the $A(\text{VO}_2)_2(\text{PO}_4)\cdot 3\text{H}_2\text{O}$ ($A=\text{K}^+$, NH_4^+ and Rb^+) materials. The SHG measurements were performed at 80K in order to higher the laser damage thresholds. A little degradation occurred even by using a low incident energy (fundamental energy = 28 mJ). Even if a decrease of the signal was observed after the first measurements, it was possible to compare the SHG responses: At 532 nm, the response of K, NH_4 and Rb analogues are about 24, 6 and 2 times stronger than that of quartz (Figure 5). The evolution of the SHG response for different cations in our chiral inorganic structures cannot be compared with the one of previously reported polar inorganic structures. Firstly, the polarizability of the cations in our structures plays no role on the SHG response since the intensity is lower when the alkali metal is more polarizable. Moreover, the dimensionality which is identical in the three materials cannot be a factor influencing the NLO properties. In addition, the Cheng's theory cannot be used because the materials are not polar (the net dipole moments cancel each other in chiral $P2_12_12_1$ space group). All these features which are specific of polar materials can also not be used to understand the relationships between the chirality and the SHG performances. Moreover, the NLO property cannot be related to the distortion of the centrosymmetry. Hence, the distortion of the $A(\text{VO}_2)_2(\text{PO}_4)\cdot 3\text{H}_2\text{O}$ ($A=\text{K}^+$, NH_4^+ and Rb^+) structures from one to the other is negligible in comparison of the distortion of this chiral structure from its pseudosymmetric centric structure.

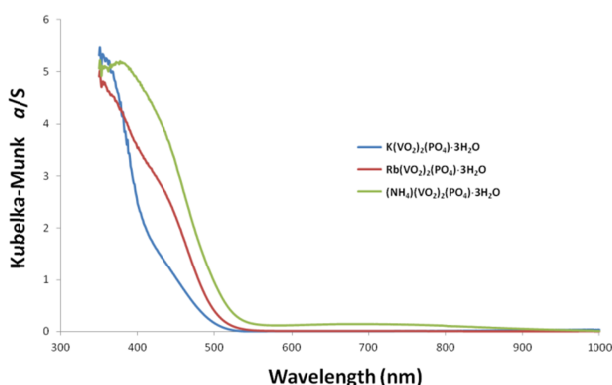


Figure 4. Diffuse reflectance spectra of compounds $A(\text{VO}_2)_2(\text{PO}_4)\cdot 3\text{H}_2\text{O}$ ($A=\text{K}^+$, NH_4^+ and Rb^+). The reflectance is converted with use of the Kubelka-Munk equation.

The main difference between the structures of $\text{K}(\text{VO}_2)_2(\text{PO}_4)\cdot 3\text{H}_2\text{O}$, $\text{NH}_4(\text{VO}_2)_2(\text{PO}_4)\cdot 3\text{H}_2\text{O}$ and $\text{Rb}(\text{VO}_2)_2(\text{PO}_4)\cdot 3\text{H}_2\text{O}$ is the volume of the unit-cells. The contraction of the structure would be at the origin of the different SHG responses. For the materials reported in this article, the more the crystal structure is contracted, the stronger the SHG response is. Thus, the SHG intensities which are 2, 6 and 24 times stronger than quartz correspond to unit-cells with V/Z of 229.46 \AA^3 (for $A=\text{Rb}$), 228.5 \AA^3 (for $A=\text{NH}_4$) and 223.71 \AA^3 (for $A=\text{K}$) respectively (Figure S3). This slight contraction of the structure would also be at the origin of this strong increase of the SHG response.

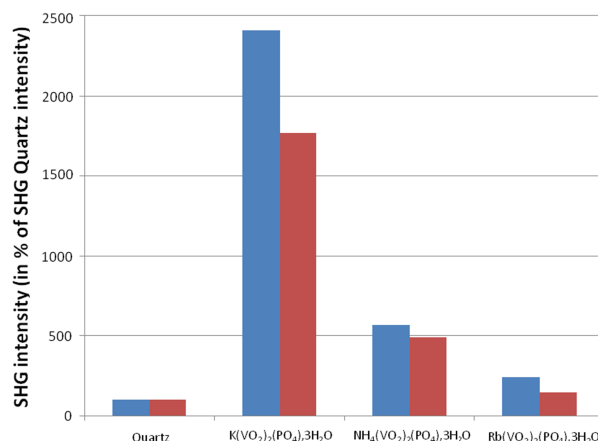


Figure 5. SHG measurements of $A(\text{VO}_2)_2(\text{PO}_4)\cdot 3\text{H}_2\text{O}$ ($A=\text{K}^+$, NH_4^+ and Rb^+) materials (First and second measurement in blue and red, respectively).

CONCLUSIONS

SHG was firstly demonstrated in 1961 in a quartz crystal.²² Since then, little effort has been realized to understand the relationships between *chiral* inorganic materials and SHG response. Thus, most of the attention has been focused on the *polar* inorganic materials but the relationships between polar structure and the NLO properties are different than for the ones of chiral structures. The determination of the crystal structure of new chiral $A(\text{VO}_2)_2(\text{PO}_4)\cdot 3\text{H}_2\text{O}$ ($A=\text{K}^+$ and Rb^+) and the SHG measurements showed that the response depends on the contraction of the structure. This observation could also be of interest for the future design and enhancement of SHG properties from chiral inorganic materials.

Acknowledgements

We thank Thierry Roisnel and the Centre de DIFfractométrie X (CDIFX), UMR 6226 "Institut des Sciences Chimiques de Rennes" for discussion regarding the crystal structures. We

would also like to thank Stéphane Grolleau for performing TGA and DSC measurements on the three compounds.

Notes and references

^a Institut des Sciences Chimiques de Rennes, UMR 6226 CNRS, Université de Rennes 1 – Ecole Nationale Supérieure de Chimie de Rennes, Avenue du Général Leclerc, CS 50837, 35708 Rennes, France.

^b Institut des Matériaux Jean Rouxel, Université de Nantes, CNRS, 2 rue de la Houssinière, 44322 Nantes Cédex 03, France.

^c PRES Normandie, Crystal Genesis Unit, SMS, EA 3233 Université de Rouen, F-76821 Mont-Saint-Aignan Cedex, France.

Electronic Supplementary Information (ESI) available: Powder X-ray diffraction patterns (Figure S1), Particle-size distribution analysis (Figure S2), SHG Intensity vs. Unit-cell volume (Figure S3) and Crystallographic data of compounds $A(\text{VO}_2)_2(\text{PO}_4)\cdot 3\text{H}_2\text{O}$ ($A=\text{K}^+$ and Rb^+) (CSD-427070 and CSD-427071, respectively).

1. N. Ye, Q. Chen, B. Wu and C. Chen, *J. Appl. Phys.*, 1998, 84, 555-558.
2. H.-S. Ra, K. M. Ok and P. S. Halasyamani, *J. Am. Chem. Soc.*, 2003, 125, 7764-7765.
3. P. S. Halasyamani, *Chem. Mater.*, 2004, 16, 3586-3592.
4. E. C. Glor, S. M. Blau, J. Yeon, M. Zeller, P. Shiv Halasyamani, J. Schrier and A. J. Norquist, *J. Solid State Chem.*, 2011, 184, 1445-1450.
5. M. D. Donakowski, R. Gautier, J. Yeon, D. T. Moore, J. C. Nino, P. S. Halasyamani and K. R. Poeppelmeier, *J. Am. Chem. Soc.*, 2012, 134, 7679-7689.
6. R. Gautier, M. D. Donakowski and K. R. Poeppelmeier, *J. Solid State Chem.*, 2012, 195, 132-139.
7. A. M. Fry, H. A. Seibel, I. N. Lokuhewa and P. M. Woodward, *J. Am. Chem. Soc.*, 2012, 134, 2621-2625.
8. R. Gautier and K. R. Poeppelmeier, *Inorg. Chem.*, 2012, 51, 10613-10618.
9. A. M. Fry and P. M. Woodward, *Crystal Growth & Design*, 2013.
10. R. Gautier and K. R. Poeppelmeier, *Crystal Growth & Design*, 2013, 13, 4084-4091.
11. T. K. Bera, J.-H. Song, A. J. Freeman, J. I. Jang, J. B. Ketterson and M. G. Kanatzidis, *Angewandte Chemie International Edition*, 2008, 47, 7828-7832.
12. T. K. Bera, J. I. Jang, J.-H. Song, C. D. Malliakas, A. J. Freeman, J. B. Ketterson and M. G. Kanatzidis, *J. Am. Chem. Soc.*, 2010, 132, 3484-3495.
13. H. Wu, H. Yu, Z. Yang, X. Hou, X. Su, S. Pan, K. R. Poeppelmeier and J. M. Rondinelli, *J. Am. Chem. Soc.*, 2013, 135, 4215-4218.
14. A. Zayit, M. Pinsky, H. Elgavi, C. Dryzun and D. Avnir, *Chirality*, 2011, 23, 17-23.
15. L. Wilde, H. Worzala, U. Steinike and G.-U. Wolf, *Mater. Sci. Forum*, 2000, 321-324, 982-987.
16. *Nonius Kappa CCD Program Software*, Nonius BV, Delft, The Netherlands, 1998.
17. L. J. Farrugia, *J. Appl. Cryst.*, 1999, 32, 837-838.
18. A. Altomare, M. C. Burla, M. Camalli, G. Cascarano, C. Giacovazzo, A. Guagliardi, A. G. G. Moliterni, P. G. and R. Spagna, *J. Appl. Cryst.*, 1999, 32, 115-119.
19. G. M. Sheldrick, in *SHELXL-97: Program for Crystal Structure Refinement*, University of Gottingen, Gottingen, Germany, 1997.
20. S. K. Kurtz and T. T. Perry, *J. Appl. Phys.*, 1968, 39, 3798-3813.
21. P. S. Halasyamani and K. R. Poeppelmeier, *Chem. Mater.*, 1998, 10, 2753-2769.
22. P. A. Franken, A. E. Hill, C. W. Peters and G. Weinreich, *Phys. Rev. Lett.*, 1961, 7.